15A.3 WIND GUST SPEED ANALYSIS IN RTMA

Yanqiu Zhu,* Geoff DiMego, John Derber, Manuel Pondeca,
Geoff Manikin, Russ Treadon, Dave Parrish, Jim Purser

NOAA/NWS/NCEP/Environmental Modeling Center, Camp Springs, Maryland

1. INTRODUCTION

The Real-Time Mesoscale Analysis (RTMA, De Pondeca et al. 2007, Pondeca and Manikin, 2009) is a NOAA-NWS gridded surface analysis system developed at the Environmental Modeling Center (EMC) of the National Centers for Environmental Prediction (NCEP) in collaboration with the Global Systems Division (GSD) of the Earth System Research Laboratory (ESRL). Based on the 2DVAR-version of Gridded Statistical Interpolation (GSI, Wu et al. 2002), the RTMA generates hourly National Digital Forecast Database (NDFD)-matching analyses and estimates of analysis uncertainty for near-surface temperature, wind and moisture for domains covering Continental United States (CONUS), Alaska, Hawaii and Puerto Rico (Guam is coming soon). The CONUS region is the focus of this paper where a downscaled 1-hour Rapid Update Cycle (RUC) forecast (Benjamin et al. 2004) is used as first guess.

With its capabilities of being real-time and in high spatial and temporal resolutions, one of RTMA's important applications is to provide a comprehensive set of analyses for potential severe weather events, such as high winds and gusts. Wind gust is an important and challenging forecast element, and it was made the 11th NDFD element to become operational in the NDFD in 2007. In alignment with efforts on providing gust forecasts/guidance products (e.g., Glahn and Dallavalle 2005), it is our goal to add wind gust analysis to RTMA. For CONUS, the wind gust analysis is on a NDFD-resolution 5-km grid and will be used to verify gust forecasts and monitor hazardous weather events.

This paper will cover the following tasks: adding wind gust speed as a new control variable in the GSI and RTMA, examination of the gust observations from various sources, especially mesonet data, and generation of test analyses over the CONUS region.

*Corresponding author address: Yanqiu Zhu, EMC/SAIC, 5200 Auth Road, Camp Springs, MD 20746-4304; email: Yanqiu.Zhu@noaa.gov.

2. WIND GUST SPEED ANALYSIS

The RTMA has been providing high resolution analyses for surface pressure, 10m wind, 2m temperature and moisture over CONUS on the 5-km NDFD grid since August 2006. The background fields for the analyses are generated from RUC 1-hour forecasts at 13-km horizontal resolution downscaled to a 5-km NDFD grid (Benjamin et al. 2007). The discrepancies between the observations and the background fields are spread out from the observation locations through the background error covariances. Isotropic background error covariances were constructed from numerical recursive filters by Purser, et al. (2003a); Later, a unique aspect of the RTMA, terrain-following anisotropic background error covariances, were implemented to take into account the topographic effect (Purser et al. 2003b, Purser 2005, and De Pondeca et al. 2007). Analyses are produced at every hour using land synoptic, METAR, ship, buoy, tide gauge, C-MAN and mesonet observations of surface pressure, temperature, wind and/or moisture, as well as satellite estimates of oceanic surface wind from SSM/I and QuickSCAT. To be considered for inclusion in the RTMA analysis, observations must be available at NCEP by 25 minutes past the hour. Conventional observations must have an observation time within 12 minutes of the analysis time whereas satellite estimates must be within 90 minutes of analysis time.

The first step of performing the wind gust speed analysis was to add gust speed as a new control variable in the RTMA. Since other variables will be added in the future for RTMA and other GSI application, effort was spent in generalizing the treatment of control variables in GSI. Exploiting the enhanced flexibility of the GSI to add/remove control variables, the gust speed variable was incorporated, and a univariate gust analysis became possible. Before we examine this analysis, we first take a look at the observations.
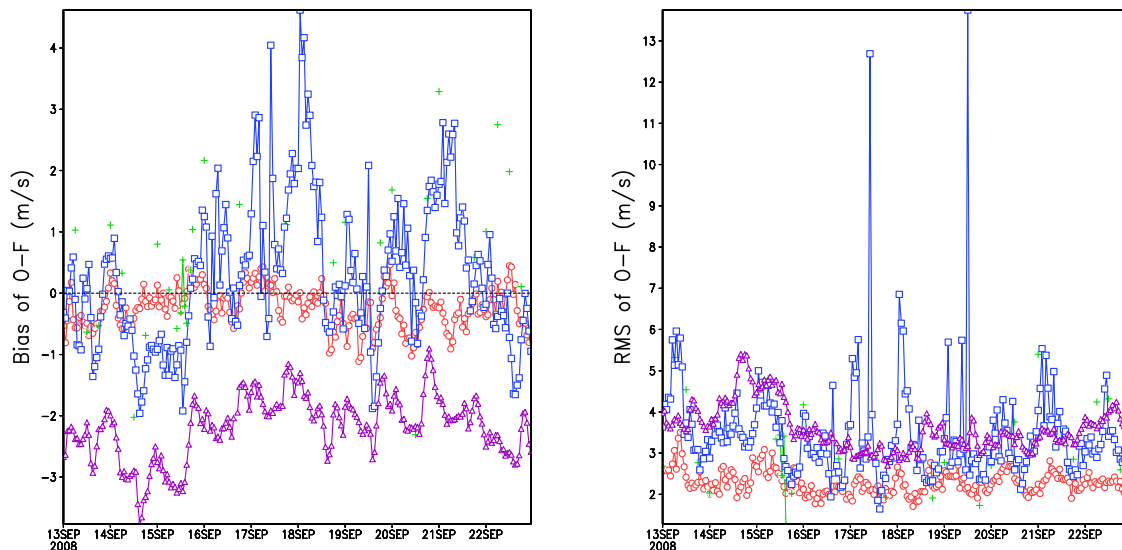
Figure 1: Time series of bias (left panel) and RMS (right panel) of gust O-F from each data source in the period of Sept. 13 to 22, 2008. Red is surface marine data (Type 180), green is METAR data (Type 181), blue is METAR data (Type 187), and purple is mesonet data (Type 188).

2.1 GUST DATA CHARACTERISTICS

The wind gust data used in this study were surface marine data (T180), surface land METAR data with reported station pressure (T181), surface land METAR data without reported station pressure (T187), and mesonet data (T188). Due to the uncertainty of instrument positioning with many mesonet data, the large volumes of this data type posed a big challenge in producing wind gust analysis. Despite this limitation, we hoped that mesonet gust data would have a positive impact on the analysis (especially where other gust data were not available) by applying the provider and the station-by-station use and reject lists for mesonet wind data provided by GSD and the Weather Forecast Offices. The compatibility of the gust data from various sources was the main focus in this work, and the applicability of the mesonet use and reject lists to mesonet gust data was also examined. The primary measures of compatibility used here were bias and root mean squared (RMS) values of the discrepancies between observations and the guess/analysis values at observation locations (O-F/O-A). One thing we also would like to point out here is that the gust guess provided by RUC is actually a gust potential product, since it is not really trying to make an accurate representation of what the gust field will look like. Instead, its intent is to predict the maximum amount of momentum that could be mixed to the surface if full mixing and momentum exchange occur.

Wind gust speed observations in an arbitrary time period of Sept. 13 to 22, 2008 were analyzed in the CONUS region. A close look at daily minimum values of gust data from different sources indicated slightly different reporting practices. The minimum values reported in METAR data were $7.2m/s$ on most of days with a few $4.1m/s$, while the minimum values of mesonet gust data were zero.

Comparisons of bias and RMS of O-F are presented in Fig. 1. Note that quality control was not applied to the gust data for this calculation; all available gust data were included. For this period, surface marine gust data had the smallest bias and RMS of O-F, while mesonet gust data had a significant negative bias and the largest RMS of O-F. This result agreed well with other studies on the quality of mesonet wind data (Pondeca et al. personal communication).

In order to examine the geographic pattern of bias, the O-F bias of each observation station was computed from all gust data sources. 2D distributions of O-F bias for all gust data sources are presented in Fig. 2. Consistent with previously mentioned time series results of O-F bias
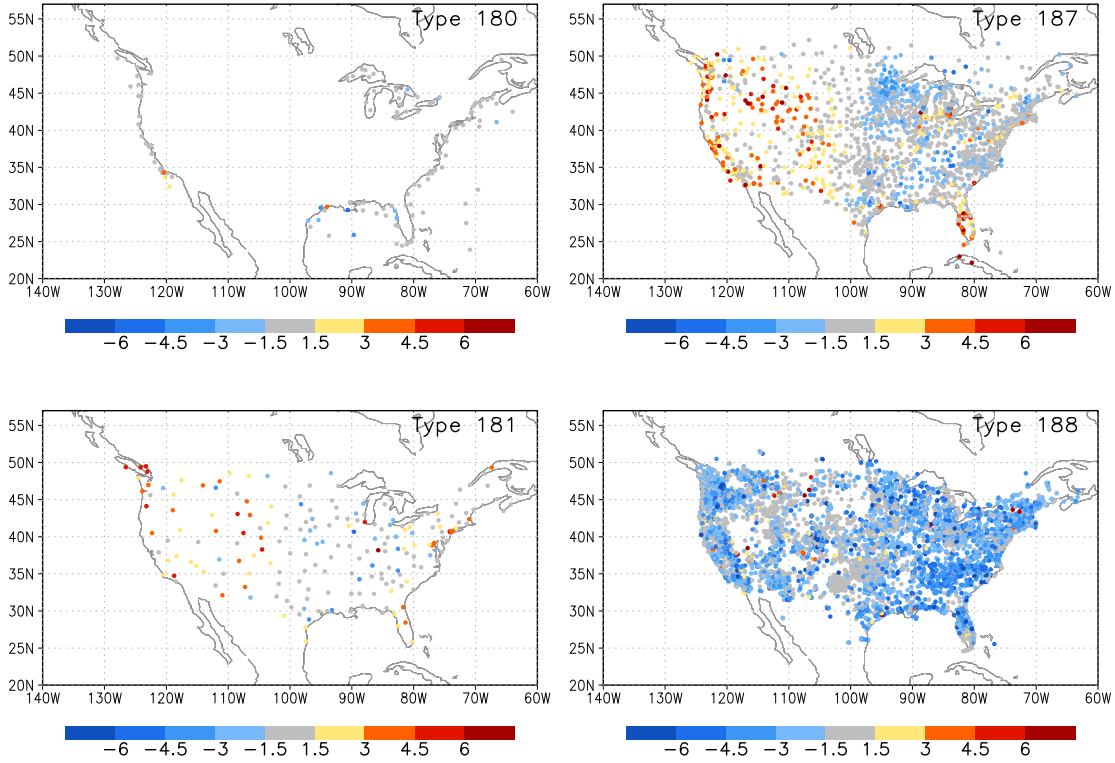
Figure 2: 2D bias features of gust O-F for each data source in the period of Sept. 13 to 22, 2008 (units are m/s).

Table 1: Statistics of mesonet gust data in the period of Sept. 13 to 22, 2008 before applying mesonet use and reject lists. The percentage values are with respect to the total number of mesonet gust data during this period.

Statistics	Obs$< 4.1m/s$	$4.1m/s \leq$ Obs $< 7.2m/s$	Obs $\geq 7.2m/s$
Mean of obs (m/s)	1.556	5.482	10.021
Bias of O-F (m/s)	-2.806	-1.014	0.237
RMS of O-F (m/s)	3.747	2.914	4.288
Obs Number (%)	1399838 (71.7%)	386681 (19.8%)	165426 (8.5%)

Table 2: Same as Table 1 except that after applying mesonet use and reject lists.

Statistics	Obs$< 4.1m/s$	$4.1m/s \leq$ Obs $< 7.2m/s$	Obs $\geq 7.2m/s$
Mean of obs (m/s)	2.057	5.511	9.883
Bias of O-F (m/s)	-2.108	-0.800	-0.053
RMS of O-F (m/s)	3.152	2.633	3.636
Obs Number (%)	510445 (26.2%)	226290 (11.6%)	109756 (5.6%)

(Fig. 1), surface marine gust data once again exhibited small bias at individual observation sites. For METAR gust data, which were over land, the results revealed overall negative O-F bias over relatively flat U.S. eastern regions except Florida, but positive O-F bias over elevated western regions. In other words, if the METAR data were assumed to be reliable, the RUC gust potential product overforecasted the gust speeds in the eastern regions while it under-forecasted the speed in western regions and in Florida. However, when we move to mesonet gust data, a very different bias pattern presented itself. Negative bias of O-F was the dominant feature everywhere for mesonet gust data. The O-F bias discrepancy pattern between mesonet and METAR poses a challenge in analyzing gust data, and differences between station elevations and model topography (Figure not shown) further complicated our effort.

To obtain a fair comparison with METAR data, the mesonet gust data was broken down into three interval bins: gust data value $\geq 7.2m/s$, $< 4.1m/s$, and in between. Tables 1 and 2 summarize the bias and RMS of mesonet gust O-F before and after applying mesonet use and reject lists, respectively. The percentages of mesonet gust data with a magnitude below $4.1m/s$ were 71.7%/26.2% of total 1951945 mesonet gust data before/after using mesonet use and reject lists, the percentages for gust data larger than or equal to $4.1m/s$ but less than $7.2m/s$ were 19.8%/11.6%, and the percentages for gust data larger than $7.2m/s$ were 8.5%/5.6%. Only a total of 43.4% of 1951945 mesonet gust data remained after applying mesonet use and reject lists. The results revealed that the mesonet use and reject lists acted as a filter where stations with very large O-F biases were excluded, but the basic underlying bias patterns still remained. The biases for intermediate and strong gust data looked reasonable, but the large RMS and negative bias associated with weak gusts were quite alarming compared with the small mean of these gust magnitudes.

The bias at each observation station for gust data is displayed in Fig. 3 after applying use and reject lists. When only weak gust ($< 4.1m/s$) data were included in the calculation, stations with large negative biases were present throughout the CONUS region regardless of whether use and reject lists were applied. On the other hand, when only strong gust ($\geq 7.2m/s$) data were included, one interesting pattern emerged – many stations had large positive biases in the western areas but negative biases in the eastern areas, which was very similar to the bias pattern of METAR gust data. The relatively small biases shown in Tables 1 and 2 for strong gusts were actually because the eastern and western biases canceled out each other. The pattern leaned toward negative bias when only gust data between $4.1m/s$ and $7.2m/s$ were included.

2.2 GUST DATA UTILIZATION

From the assessment of gust data from various data sources in previous section, it was seen that surface marine gust data had the smallest bias and RMS of O-F. While mesonet gust data with strong gusts displayed a similar bias pattern as METAR gust data, mesonet gust data with weak gusts showed significant negative bias. Since it was difficult to determine whether the negative bias associated with weak mesonet gusts was caused by gust background or gust observations, an experiment was carried out to investigate the impact of mesonet gust data with weak gusts. More details will follow in this regard.

In addition to the gross-error check performed inside GSI, several rules were followed in the handling of gust data. For the observations that were at the same location, the one that was closest to the analysis time was chosen. Observation error was inflated based on the report time relative to the analysis time. In this way, less weight was given to the observations that were far away from the analysis time. Moreover, the discrepancy of observation station elevation and model surface elevation was taken into account. For mesonet gust data, observation height was assumed to be at 10m above the observation station, and mesonet use and reject lists were applied to the data. The pre-specified gust observation errors were $1.8m/s$ for surface marine and METAR data, and $4.5m/s$ for mesonet data, and the background error variance was $3.0m/s$. Gust background error correlation length was chosen to be comparable to that of the 10m wind analysis in the current RTMA.

Three sets of experiments were conducted for gust data analysis in the RTMA for the time period of Sept. 13 to 22, 2008:

- Exp. 1: used only surface marine and METAR data;

- Exp. 2: used only surface marine and mesonet data with all mesonet data given the same observation error;

- Exp. 3: used surface marine, METAR and mesonet data, but observation error was inflated for mesonet data that were less than $7.2m/s$.
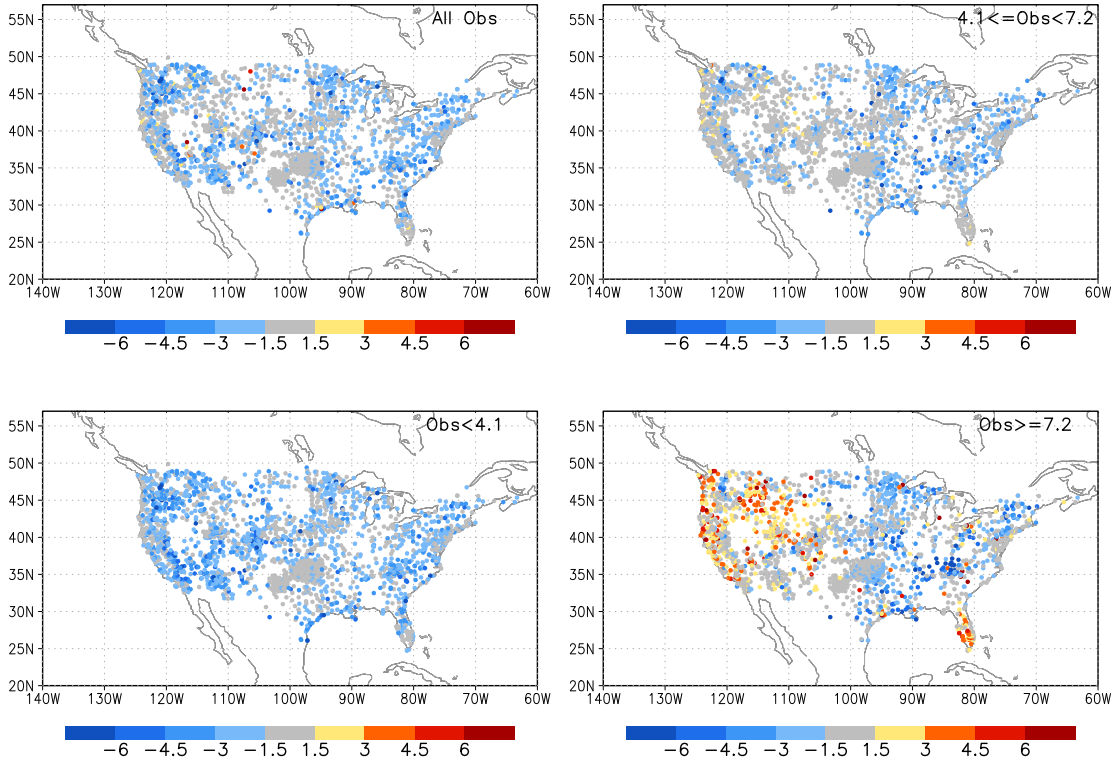
Figure 3: 2D O-F bias patterns of break-down mesonet gust data after applying mesonet use and reject lists in the period of Sept. 13 to 22, 2008 (units are m/s): All remaining data (upper left), data $< 4.1m/s$ (lower left), $4.1m/s \leq$ data $< 7.2m/s$ (upper right), and data $\geq 7.2m/s$ (lower right).

Table 3: Bias and RMS of gust O-F‖O-A for Exp. 1

Statistics	surface marine	METAR(T181)	METAR(T187)	mesonet
Bias of O-F (m/s)	-0.240‖-0.070	0.553‖0.326	-0.250‖-0.086	-2.176‖-2.166
RMS of O-F (m/s)	2.304‖0.913	3.247‖1.358	3.333‖1.656	3.620‖3.553

Table 4: Bias and RMS of gust O-F‖O-A for Exp. 2

Statistics	surface marine	METAR(T181)	METAR(T187)	mesonet
Bias of O-F (m/s)	-0.240‖-0.060	0.553‖1.107	-0.250‖0.523	-2.176‖-1.567
RMS of O-F (m/s)	2.304‖0.908	3.247‖3.193	3.333‖3.008	3.620‖2.942

Table 5: Bias and RMS of gust O-F‖O-A for Exp. 3

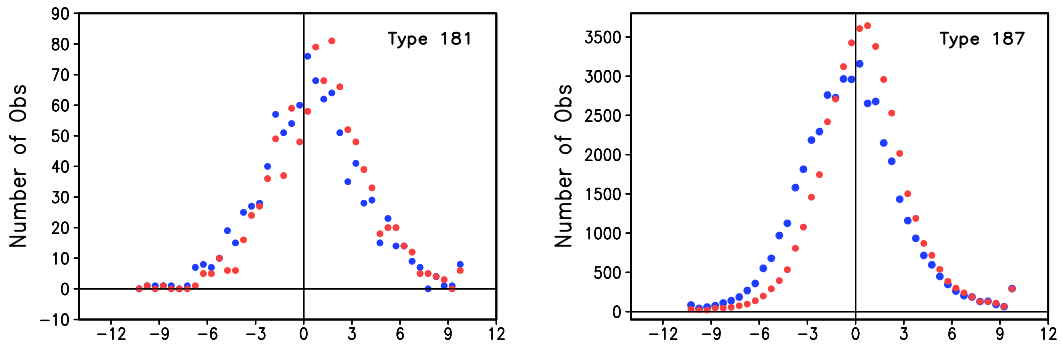| Statistics	surface marine	METAR(T181)	METAR(T187)	mesonet
Bias of O-F (m/s)	-0.237‖-0.069	0.512‖0.340	-0.300‖0.096	-1.464‖-1.285
RMS of O-F (m/s)	2.258‖0.815	3.161‖1.141	3.086‖1.189	3.020‖2.640

Figure 4: Histograms of O-F (blue dots) and O-A (red dots) for METAR gust data in Exp. 2 for the period of Sept. 13 to 22, 2008.

The bias and RMS of O-F and O-A are summarized in Tables 3, 4 and 5 for the three experiments, respectively. Since mesonet gust data were not used in Exp. 1 and METAR gust data were not used in Exp. 2, the statistics shown for these two experiments included all gust data of each data source. However, the statistics shown for Exp. 3 included only gust data that passed quality control.

In Exp. 1, both bias and RMS of O-A of surface marine and METAR gust data were improved compared with their bias and RMS of O-F, and the comparable or slightly better O-A versus O-F of mesonet gust indicated that the assimilation of surface marine and METAR gust data did not degrade the overall fit of gust field to mesonet gust data, though mesonet gust were not used in generating the gust analysis.

Exp. 2 was performed to address the impact of mesonet gust data with weak gust magnitudes. In Exp. 2, the fits of gust analysis to surface marine and mesonet gust data were better than the fits of gust guess field to these data, but the biases of O-A for METAR gust data became worse than their biases of O-F for both Types 181 and 187. It was believed that the gust analysis field was pushed lower at many mesonet gust data sites and their vicinities due to the negative biases of O-F from large amounts of mesonet gust data with weak gusts, and this resulted in higher positive bias of O-A for METAR gust data. This process can also be illustrated in terms of histograms of METAR gust O-F and O-A (Fig. 4). Compared with O-F distributions, O-A histograms of both Types 181 and 187 shifted to the (further) positive side. Additional experimentations showed that this negative impact on the fit to METAR data could be alleviated by inflating the observation errors of weak mesonet gust data. These results for Exp. 2 implied the incompatibility between METAR gust data and weak mesonet gust data.

To minimize the detrimental impact from weak mesonet gust data on the gust analysis while keeping weak mesonet gust data in the analysis process, the observation errors of these data were inflated in Exp. 3. We tried to strike a balance between compatibility of assimilating gust data from different sources and allowing mesonet gust data to provide complementary information, especially in domains where other data were not available. From Table 5 it is seen that the fits of gust analyses to gust observations were better than the fits of gust guess to gust observations for all data sources. The daily evolution of quality-controlled O-F and O-A RMS (Fig. 5) for METAR (left panel) and mesonet (right panel) gust data also confirmed the improvement of gust analysis over gust guess field. A close examination of gust analysis increments also found that the results of Exp. 3 were in line with those of Exp. 1. The data impact on small scale structure will be discussed with a case study in the next section.

3. CASE STUDY

One of the important applications of the RTMA is to provide a comprehensive set of analyses for the potential severe weather events at high spatial and temporal resolution. Hazardous high wind and gust events often cause hundreds of millions dollars of losses. As an example, on Dec. 31, 2008, a low pressure system moving out of the Mid-Atlantic deepened rapidly off the east coast. The passage of a cold front extending southward from this low brought strong northwesterly winds to Maryland,
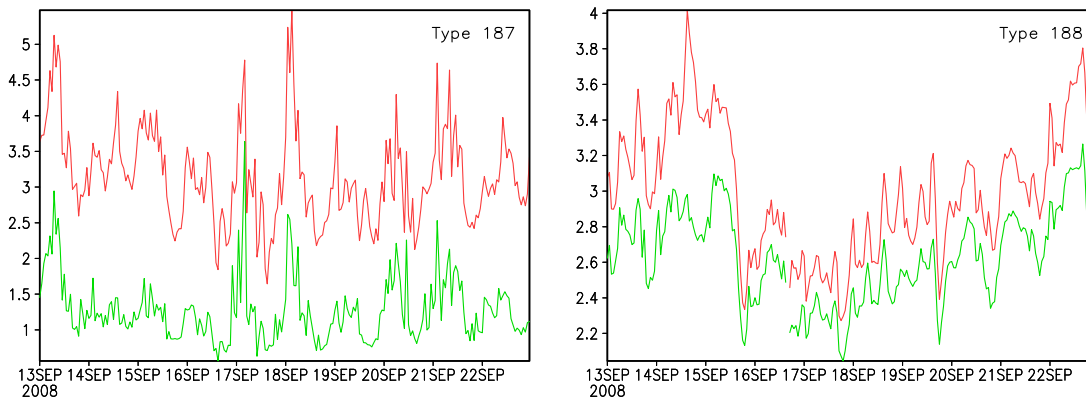
Figure 5: Time series of quality-controlled O-F (red line) and O-A (green line) RMS for METAR (left panel) and mesonet (right panel) gust data in the period of Sept. 13 to 22, 2008 (units are m/s).

Washington D.C., and Virginia areas. Wind gusts greater than $19m/s$ were observed at DCA, IAD and BWI airports. Damage caused by downed trees and powerlines was reported throughout this region as a result of sustained high winds and gusts.

Fig. 6 shows the distributions of METAR (left panel) and mesonet (right panel) gust observations used in producing gust analysis at 1500Z. Plenty of METAR and mesonet gust data were present and passed into the analysis system, including several low mesonet gust data though they will be assigned a small weight based on the data usage rules mentioned above. Compared with gust observations, gust background (Fig. 7, left panel) was seen to be over-estimated in most of this area, with over $21m/s$ of gusts over a large area stretching from Pennsylvania across Maryland, and going into the north and west of Virginia. Combining the background and observation information, gust analysis (Fig. 7, right panel) was shown improved over the background field, in particular, small scale features were evident. The areas with $21+m/s$ of gusts were greatly reduced, one of which was mainly confined to the Chesapeake Bay. Moreover, a relatively low gust area was extended southward near the stateline of Maryland and Delaware. As the pressure gradient strengthened, the gust analysis at 1800Z (Fig. 8) showed the strong gusts in the mid-Atlantic region wind field with much greater detail.

4. CONCLUSIONS AND FUTURE WORK

In this work, a wind gust speed variable was added to the RTMA as a new control variable, and gust data from surface marine, METAR, and mesonet were examined and assimilated for an arbitrary time period from Sept. 13 to 22, 2008. Due to their distinct characteristics of O-F biases, compatibility of different gust data became the main focus of this work. Among all of the gust data, surface marine data showed reasonably good O-F bias, METAR and strong mesonet gust data exhibited a pattern with negative bias over eastern regions except Florida and positive bias over western regions, while weak mesonet gust data had a significant negative bias over the CONUS. Further experimentation indicated negative impact of mesonet gust data on gust analysis when weak mesonet gust data were given the same weight as strong mesonet gust data. Therefore, small weights were assigned to weak mesonet gust data in gust analysis in order to minimize their detrimental effect.

Another challenge we faced was the uncertainty of mesonet gust data. Our results confirmed the applicability of mesonet use and reject lists to mesonet gust data; stations with very large O-F departures were excluded though fundamental bias pattern were unchanged. For gust analysis experiments conducted in this work, the gust background was provided by RUC 1-hour forecast downscaled from 13km to 5km, gust background correlation length was chosen to be comparable to that of 10m wind, and the resultant fit of gust analysis to gust observations was shown to be better than the fit of gust background to gust observations in terms of both bias and RMS. A case study was also performed for a high wind and gust event. It was seen that gust background over-forecasted in most of the relevant
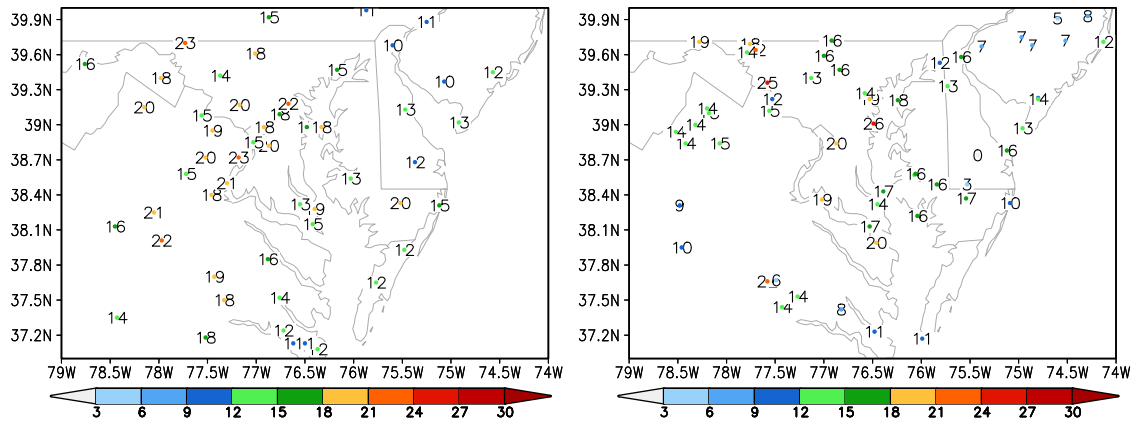
Figure 6: METAR (left panel) and mesonet (right panel) gust data distribution at 1500Z Dec. 31, 2008 (units are m/s).
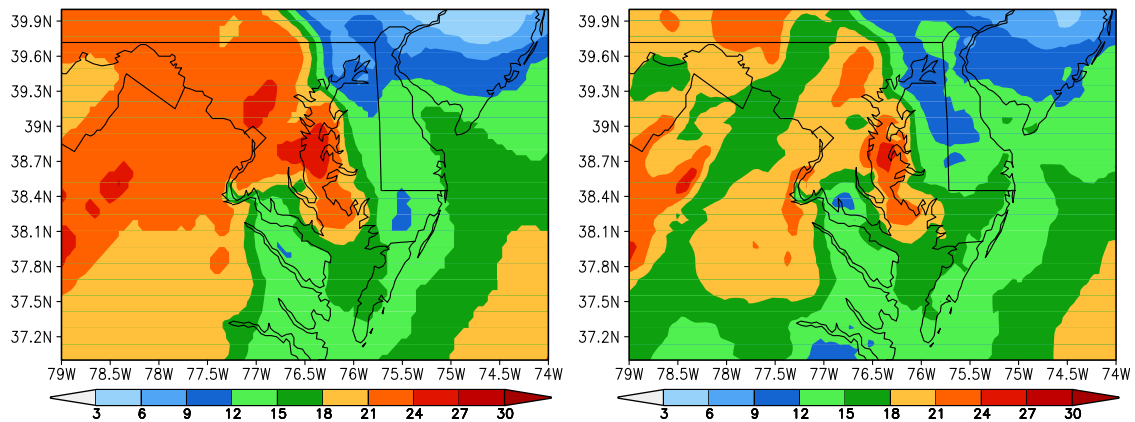

Figure 7: Gust background (left panel) and analysis (right panel) at 1500Z Dec. 31, 2008 (units are m/s).

area, and that the use of gust data led to significant improvement of the gust field with detailed small scale features.

Although important progress has been made on gust analysis, there is still room for further development. It is necessary to conduct routine gust analysis in order to refine parameters involved in the RTMA, such as wind gust correlation length, observation error, relative contribution of isotropic and anisotropic portions to the aspect tensor, etc. Moreover, more attention needs to be placed on quality control of gust data and the creation of the background field. We hope that a mechanism will be added in the gust analysis to remove gust data of poor quality based on wind data information, and

that variational quality control will be tested on gust data to adaptively update the data selection process. Bias correction of the gust background will also be explored in the future.

REFERENCES

Benjamin, S.G., D. Devenyi, S.S. Weygandt, K.J. Brundage, J.M. Brown, G.A. Grell, D. Kim, B.E. Schwartz, T.G. Smirnova, T.L. Smith, and G.S. Manikin, 2004: An hourly assimilation/forecast cycle: The RUC. *Mon. Wea. Rev.*, **132**, 495-518.

Benjamin, S. , J.M. Brown, G. Manikin and G. Mann, 2007: The RTMA Background - Downscaling of RUC data to 5 km Detail. *23rd Conf. on IIPS*,
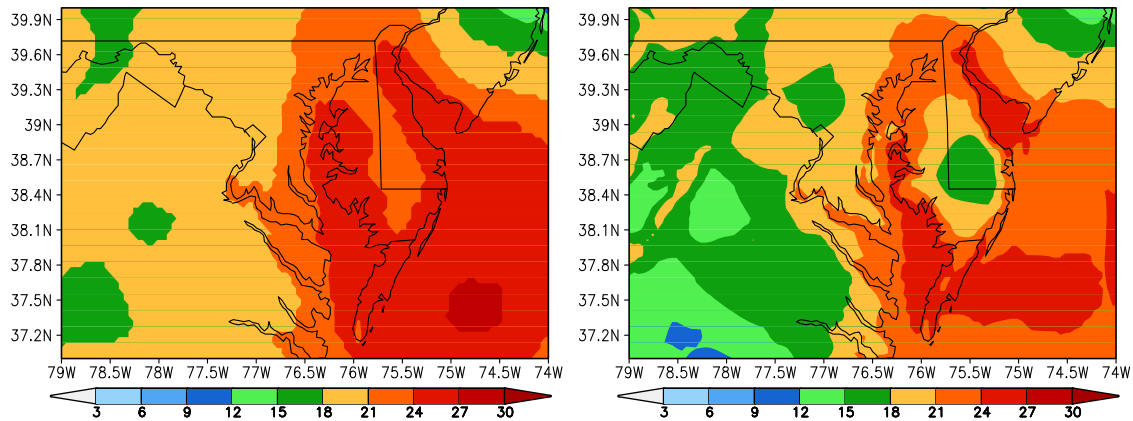
Figure 8: Gust background (left panel) and analysis (right panel) at 1800Z Dec. 31, 2008 (units are m/s).

January, 2007, San Antonio, TX, Amer. Meteo. Soc., P1.11.

Glahn, H.R., and J.P. Dallavalle, 2005: Gridded MOS - Techniques, Status, and Plans. *18th Conf. on Probability and Statistics in the Atmospheric Sciences*, Atlanta, GA, Amer. Meteor. Soc., 2.1.

De Pondeca, M. and G. Manikin, S.Y. Park, D.F. Parrish, W.S. Wu, G. Dimego, J.C. Derber, S. Benjamin, J.D. Horel, S.M. Lazarus, L. Anderson, B. Colman, G.E. Mann, and G. Mandt, 2007: The development of the real time mesoscale analysis system at NCEP. *23rd Conf. on IIPS*, San Antonia, TX, Amer. Meteor. Soc., P1.10.

Pondeca, M. and G. Manikin, 2009: Recent improvements to the Real-Time Mesoscale Analysis (RTMA). *23rd Conf. on Weather Analysis and Forecasting/19th Conference on Numerical Weather Prediction*, Omaha, NE, June, 2009, Amer. Meteo. Soc.

Purser. R.J., 2005: A geometrical approach to the synthesis of smooth anisotropic covariance operators for data assimilation. NOAA/NCEP Office Note 447, 60pp.

Purser, R. J., W. Wu, D. F. Parrish, and N. M. Roberts, 2003a: Numerical aspects of the application of recursive filters to variational statistical analysis. Part I: spatially homogeneous and isotropic Gaussian covariances. *Mon. Wea. Rev.*, **131**, 1524-1535.

Purser, R. J., W. Wu, D. F. Parrish, and N. M. Roberts, 2003b: Numerical aspects of the application of recursive filters to variational statistical analysis. Part II: spatially inhomogeneous and anisotropic Gaussian covariances. *Mon. Wea. Rev.*, **131**, 1536-1548.

Wu, W., R. J. Purser, and D. F. Parrish, 2002: Three dimensional variational analysis with spatially inhomogeneous covariances. *Mon. Wea. Rev.*, **130**, 2905-2916.